Luminescence, color and fission track zoning in apatite crystals of the Panasqueira tin-tungsten deposit, Beira-Baixa, Portugal[1]

CRAIG KNUTSON,[2] DONALD R. PEACOR AND WILLIAM C. KELLY

Department of Geological Sciences
The University of Michigan, Ann Arbor, Michigan 48109

Abstract

Concentric growth zoning of apatite crystals from the hydrothermal tin-tungsten veins of Panasqueira, Portugal, is evidenced by variations in color, fission track density and luminescence intensity. The zoning was studied to determine its chemical controls and to evaluate its potential as a stratigraphic tool for paragenetic analysis and the correlation of veins.

The apatites vary from green to colorless probably as a result of interaction between a green-producing chromaphore (most probably Fe^{2+}) and REE decolorizing agents (possibly Nd^{3+} and Ce^{3+}). Fission track density is proportional to uranium concentration. The luminescence is yellow-orange and is characterized by four emission bands whose intensities were related to chemical concentrations by linear regression. The following activation models are proposed for three of these bands: (1) 349 nm emission (bandwidth 40 nm). REE (Ce^{3+}) activation, (2) 445 nm emission (bandwidth 40 nm). REE (Eu^{2+}) activation, (3) 555 nm emission (bandwidth 100 nm). Mn^{2+} activation sensitized by Eu^{2+} and Ce^{3+}. The activation mechanism for the fourth band at 701 nm (bandwidth 50 nm) is unknown. The intensities of bands 1, 2 and 3 have a high degree of cross-correlation, and appear to be unrelated to band 4.

Logging of emission intensity and fission track density across primary growth zones defines a highly detailed "stratigraphy" for every crystal. Crystals from the same vug or the same mine pillar show strikingly similar "stratigraphies", but the maximum distance over which correlations can be demonstrated is only about ten meters.

Introduction

Apatite crystals from the tin-tungsten mining district of Panasqueira, Portugal are well known for their large size, perfection of form and conspicuous growth zoning as expressed by color, luminescence and fission track density. The apatite occurs sporadically in a large system of numerous, near-horizontal, hydrothermal veins which has been mined with continuity over an area of approximately 8 square kilometers. The geometry and interconnections of these flat veins are complex, and it is difficult to correlate individual structures from place-to-place in the large mine (Thadeu, 1951; Kelly and Rye, 1979). If the detailed growth zoning sequences ("stratigraphies") in the apatites could be correlated over large distances, space-time relationships of the vein paragenesis might be better established. Such growth zoning sequences have been documented in other systems (e.g. Roedder, 1969; Barton et al., 1977; McLimans et al., 1980), demonstrating their value in correlating space-time relations.

Several authors (Bloot and de Wolf, 1953; Gaines and Thadeu, 1971; Kelly and Rye, 1979; Kelly and Wagner, 1977) have described and studied the Panasqueira apatites. There is little agreement among theories proposed (Lagerwey, 1977; Leckebusch, 1979) to relate crystal-chemical variation and the observed color luminescence and fission track zonation. To better understand the potential and meaning of observed temporal "stratigraphy", we have examined the crystal-chemical controls of zonation by studying a single, representative Panasqueira apatite crystal. Attempts were then made to correlate these controls among crystals from different locations in the vein system. The results of this investigation are presented in four separate sections: (1) crystal-chemical control of luminescence, (2) fission track production, (3) color and (4) "stratigraphic" correlation of crystal zonation patterns. Apatite in the Panasqueira district displays different colors and forms platy, hexagonal prisms with large basal faces. This study is concerned with the most common, green to colorless variety that is associated with the main sulfide stage of mineralization (Kelly and Rye, 1979).

Luminescence

In their investigation of a fluorescent apatite from Panasqueira, Bloot and de Wolf (1953) correlated high manganese concentrations with strong fluorescence. Electron microprobe traverses across a similar Panasqueira
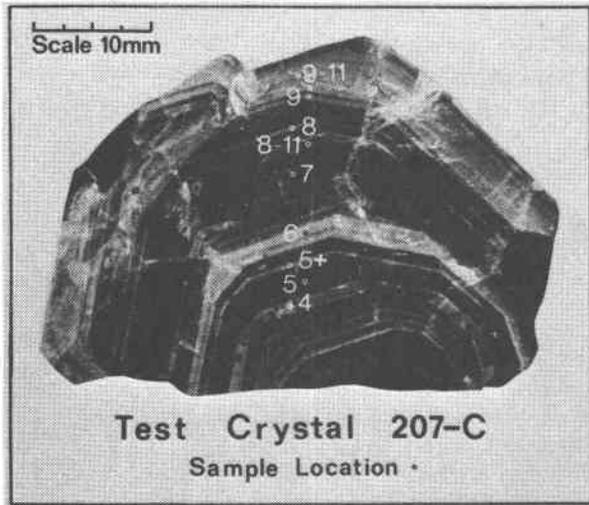
Fig. 1. Luminescence banding and sample locations of the test crystal, 207-C. Excitation energy was provided by a high-pressure Hg-lamp. The photograph is of visible light.

apatite by us and by Leckebusch (1979) failed to confirm this correlation. In this study, luminescence and absorption spectra of various zones of a representative crystal are compared and related to chemical analyses of these same zones. Statistical analyses determined the most probable luminescence mechanism.

Chemical analyses

The zones of the test crystal that were chemically analyzed for major and trace elements are identified in Figure 1 and analytical results are given in Table 1. Zone A, analyzed but not pictured in this view, is a bleached zone that was apparently produced by secondary alteration. Major element concentrations were determined using an ARL-EMX electron microprobe with three wavelength-dispersive spectrometers and an Ortex current digitizer to compensate for beam current fluctuations during data measurement. Standards were: apatite for Ca, P, Sr, F; synthetic tephroite for Mn, and Irving clinopyroxene for Fe. The analyses were made with a 0.02 μA-specimen current and 12 kV excitation using LiF, PET, and TAP crystal spectrophotometers. Drift, atomic number, fluoresence, and absorption corrections were applied to the raw data using the program EMPADR VII (Rucklidge and Gasparrini, 1969).

Trace element concentrations were determined by neutron activation analyses (NAA) at the Phoenix Memorial Laboratory of the University of Michigan. The samples were irradiated for 15 seconds and the induced radioactivity was analyzed using a Ge(Li) energy dispersive detector at one hour and two weeks following irradiation. Standards were the U.S.G.S. BCR-1 basalt and the U.S.G.S. GSP-1 granite (Flanigan, 1973). Analyses for Pr, Gd, Er, Yb and Y were not possible because of background interference related to the calcium in the samples. The neutron activation analyses compare well with estimates of trace

element concentrations in a representative Panasqueira apatite made by Lagerwey (1977).

Absorption spectrophotometric scans

Three zones of the test crystal, two luminescent and one without luminescence were analyzed in order to determine their absorption spectra. Radiation from a UV-hydrogen lamp transmitted perpendicular to the c-axis through 0.2 mm unpolished sections was measured with a Cary-14 double-beam spectrophotometer. Relative absorption is shown in Figure 2.

The absorption scans indicate that zone 7 absorbs relatively little UV radiation, while zones 6 and 5+ absorb a great deal. The latter two zones have high concentrations of REE (537 and 410 ppm, respectively) relative to zone 7 (56 ppm). The manganese concentrations for these zones is variable but does not relate to the degree of absorption. The results suggest that UV absorption is primarily a function of REE abundances, and that if manganese is involved it must be through a coupled reaction.

Quantification of luminescence intensity

The test crystal was excited by a filtered xenon lamp and the fluorescent emission was recorded with a Jarrel-Ash double monochromator. Filters [(NiSiO$_4 \cdot$6H$_2$O), cyanine dye and Corning glass #754] restricted the excitation energy to a 100 nm band centered at 250 nm. The luminescence spectrum is characterized by four emission bands (Fig. 3): (1) 349 nm (bandwidth = 40 nm); (2) 445 nm (40 nm); (3) 555 rm (100 nm); (4) 701 nm (50 nm). The maxima at 445 and 555 nm were previously noted in Panasqueira apatites by Lagerwey (1977) and Leckebusch (1979).

Photographic filtering techniques were used to reduce the luminescence of each of the test zones to an emission band. The ten samples analyzed by NAA were loosely packed into equal-area holes in a small, nonfluorescing carbon disc and irradiated by high-pressure Hg-lamps (short wavelength UV). The four characteristic emission bands were isolated using the following filters, and intensities were recorded photographically.

Band (1) 349 nm; Corning glass #5480, C.S. #7-60 plus-X film
Band (2) 445 nm; Kodak wratten #47 (glass) plus-X film
Band (3) 555 nm; Kodak wratten #61 (gel) plus-X film
Band (4) 701 nm; Kodak wratten #29 (gel) HIE infrared film

Measurements of reflectivity from each photographic positive allowed quantification of the emission intensities for each of the ten samples. As a consequence of the filtering techniques, reflectivity measurements can quantify emission intensity only within each characteristic emission band and not between.

In order to utilize the measurements of reflectivity from the photographs it is necessary to relate reflectivity (R_p) to the intensity of luminescence (I). The following relations, which are in part reviewed by Buerger (1960), are necessary for such a derivation: (1) $I \alpha E_n$ where E_n is exposure of the negative; (2) $D_n \alpha \log E_n$ where D_n is the density of the negative; (3) $E_p \alpha - D_n$ where E_p is exposure of the positive;

Table 1. Chemical analyses, relative emission intensities (relative reflectivity units), and fission track densities for 10 zones of the test crystal.

Zone	9	9-11	8	8-11	7	6	5+	5	4	A
Electron microprobe analyses in oxide %										
CaO	53.7		54.6		53.8	54.7	53.6	53.6	53.9	
PO3	42.5		41.9		42.5	42.8	42.1	42.4	42.0	
F=O	1.8		1.7		1.8	1.7	1.5	1.6	1.6	
MnO	0.8		1.0		1.0	0.8	2.5	2.2	2.1	
SrO	0.4		0.3		0.3	0.1	0.7	0.5	0.5	
total	99.2		99.4		99.4	100.1	100.4	100.3	100.1	
Neutron activation analyses in ppm.										
Mn	2629	2625	3768	4806	3020	2340	6393	6027	5724	2456
La	73.6±0.4	79.1±0.5	82.9±0.5	35.7±0.2	5.3±0.1	166.6±0.7	88.1±0.6	6.6±0.2	27.9±0.3	38.4±0.3
Ce	134.8±3.3	139.1±3.2	200.1±3.3	48.7±2.8	13.9±0.0	294.0±4.4	160.5±3.5	12.1±2.2	59.7±3.2	69.3±3.6
Nd	33.0±0.0	43.2±11.	78.3±12.	18.6±0.0	16.8±0.0	100.0±17.	62.9±12.	41.0±9.2	27.9±0.0	29.5±9.1
Sm	11.5±0.1	12.5±0.1	30.1±0.1	4.0±0.0	1.0±0.0	53.3±0.1	4.0±0.1	1.2±0.0	4.7±0.1	3.9±0.1
Eu	100.8±3.4	100.4±3.5	241.9±8.6	29.0±1.0	16.1±0.6	196.5±6.5	25.2±0.9	3.8±0.3	14.7±0.6	33.9±1.3
Tb	2.5±0.4	2.1±0.4	8.2±1.0	0.7±0.2	0.4±0.0	14.5±1.8	4.1±0.6	0.5±0.0	1.4±0.2	1.2±0.2
Dy	19.8	22.1	5.5	7.5	2.4	107.0	49.1	3.3	18.0	2.6
Lu	2.1±0.2	2.2±0.2	2.8±0.2	0.7±0.1	0.1±0.0	4.7±0.3	1.6±0.1	0.2±0.0	0.5±0.1	2.6±0.1
Sc	0.1±0.0	0.1±0.0	2.1±0.0	0.3±0.0	0.2±0.0	0.1±0.0	1.1±0.0	0.8±0.0	1.2±0.0	0.5±0.0
U	1.4±0.0	1.6±0.0	3.0±0.7	1.1±0.4	1.2±0.4	2.1±0.0	4.0±0.9	1.2±0.0	4.7±1.0	1.9±0.0
Th	2.8±0.5	3.7±0.5	2.0±0.0	4.6±0.4	1.2±0.0	17.2±0.8	23.3±0.7	1.5±0.0	9.3±0.5	4.4±0.5
Relative Luminescence Intensity										
Band 1	43.0	38.0	43.0	34.0	31.0	50.0	26.0	23.5	35.6	35.0
Band 2	42.5	42.5	42.5	37.5	37.5	45.0	40.0	35.0	37.5	37.5
Band 3	45.0	37.5	50.0	32.5	30.0	47.5	40.0	30.0	35.0	37.5
Band 4	36.0	35.5	47.0	29.0	34.0	26.0	31.0	32.2	30.6	42.0
Fission Track Density										
trx/mm^2	1900	1900	2280	1140	760	2130	2850	3800	3800	
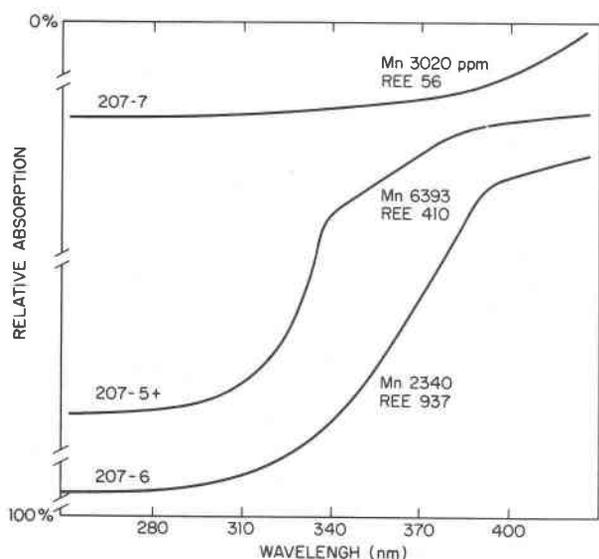
Fig. 2. Relative absorption of ultraviolet radiation by zones 7, 6, and 5+ of the test crystal.

(4) $D_p \alpha \log E_p$ where D_p is density of the positive; (5) $R_p \alpha$ (antilog $D_p)^{-1}$. Combining these functions leads directly to the relation: (6) $I \alpha R_p$; i.e., Reflectivity of the positive is proportional to luminescence intensity.

Statistical analysis

In order to determine the relations between luminescence intensity and a given activator element or elements, linear regressions were carried out. Correlation coefficients
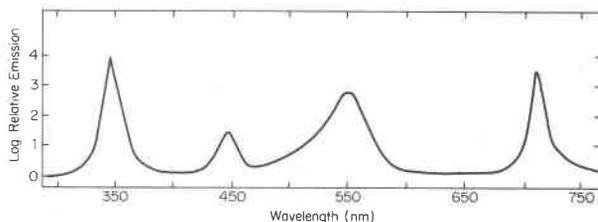
Fig. 3. Luminescence spectrum of the test crystal. Excitation energy = 250 nm (bandwidth = 100 nm).

Table 2. Correlations between film reflectivities (as recorded for the four emission bands) and element concentrations.

	Band 1 (349 nm) Rp	Band 2 (445 nm) Rp	Band 3 (555 nm) Rp	Band 4 (701 nm) Rp
Mn	-.70	-.56	-.39	-.30
La	.68	.90	.81	-.16
Ce	.74	.92	.90	-.01
Nd	.51	.71	.77	-.01
Sm	.82	.81	.78	-.06
Eu	.82	.84	.89	.36
Tb	.71	.78	.79	-.10
Dy	.50	.66	.50	-.56
Lu	.79	.84	.84	.13
Se	-.07	-.04	.33	.51

(R-values) were determined based on the assumption that a given luminescent intensity (I) is proportional to the concentration of a given element, X_i. Because I is proportional to measured reflectivities (R_p), correlations were sought between values of R_p and concentrations as determined for various crystal zones.

Correlation coefficients are listed in Table 2. Manganese correlates negatively with all emission bands. In addition, bands 1, 2 and 3 have large correlation coefficients with several rare earth elements, most notably Sm, Eu, Ce and Lu. Correlation coefficients between band 4 and all elements are either negative, or have small positive values, with the exception of Se. All of these relations will be discussed in detail below.

Table 3 lists correlation coefficients between rare earth element concentrations. Almost all coefficients are very high, as expected for rare earth elements. Only the value between Dy and Eu is markedly low. Because these coefficients are uniformly high, attempts to correlate emission bands with specific REE activators and enhancers are futile; that is, a given band may only be associated with the entire group of REE, in general.

Table 4 is the correlation matrix for film reflectivities (i.e. intensities). The correlation coefficients between bands 1, 2 and 3 are very large, implying that they have related origins. However, values between band 4, and bands 1, 2 and 3 are uniformly small, implying that they are caused by different mechanisms.

Luminescence models

The correlations described above provide evidence for the causes of the various bands. Band 3, for example, has the wavelength (555 nm) and broad shape which have been

Table 4. Correlation matrix for film reflectivities for each emission band.

	Rp-Band 1	Rp-Band 2	Rp-Band 3	Rp-Band 4
Rp-Band 1 (349 nm)	1	.82	.77	.12
Rp-Band 2 (445 nm)		1	.86	.07
Rp-Band 3 (555 nm)			1	.34
Rp-Band 4 (701 nm)				1

attributed by several authors to activation by Mn (Goldberg, 1966; Gorobets, 1968; Kallman and Spruch, 1962; Mariano and Ring, 1975; McConnel, 1963; Portnov and Gorobets, 1969; Taraschan, 1969; Weyl, 1959). In apparent contrast to this wealth of earlier research, we observe that the correlation coefficient between Mn and intensity of band 3 is negative (Table 2). On the other hand, the correlations with REE are large and positive. Our data, when combined with those of other authors, suggest a compound mechanism for luminescence. The most probable mechanism is one in which Mn acts as the activator, as suggested by other authors, but in which incident ultraviolet radiation is first absorbed by REE. It is subsequently transferred to Mn by resonant processes. Mechanisms of this kind are quite common in inorganic solids containing REE (Botden, 1952; van Uitert, 1966).

Emission bands 1 (349 nm) and 2 (445 nm) are also related to REE (Table 2). Portnov and Gorobets (1969) and Botden (1952) have studied synthetic F-apatites activated by different REE. Emissions resulting from f-orbital transitions have the approximate wavelengths of bands 1 and 2. Emission at approximately 350 nm is attributed to Ce^{3+}, and emission at approximately 450 nm is attributed to Eu^{2+}. As seen in Table 5, Ce and Eu do not have the highest correlation with Rp-1 and Rp-2, but they are certainly valid models considering the high degree of correlation among the REE. Because Eu and Ce are the REE exhibiting primary emissions, we postulate that they are also the REE involved in the sensitized luminescence of band 3-Mn emission. The correlation coefficients for Eu and Ce to Rp band 3 (Table 5) support this model.

The intensity of band 4 (701 nm) correlates poorly with the other emission bands and with all of the analyzed elements in the apatite (Tables 2 and 3). The peak shape (Fig. 3) is similar to those of bands 1 and 2, suggesting a similar f-orbital transition involving a REE, but the lack of correlations suggests that a different mechanism may be respon-

Table 3. Correlation matrix for REE concentrations.

	La	Ce	Nd	Sm	Eu	Tb	Dy	Lu	Se
La	1	.98	.86	.85	.72	.89	.87	.89	-.01
Ce		1	.91	.90	.84	.93	.80	.91	.13
Nd			1	.87	.78	.76	.76	.79	.30
Sm				1	.88	.97	.76	.87	.06
Eu					1	.82	.42	.80	.29
Tb						1	.82	.85	.15
Dy							1	.70	-.21
Lu								1	.03
Se									1

Table 5. Elements having the highest correlations (R-values) with the film reflectivities for each emission band.

Rp-Band 1 (349 nm)	Rp-Band 2 (445 nm)	Rp-Band 3 (555 nm)	Rp-Band 4 (701 nm)
Eu (.82)	Ce (.92)	Ce (.90)	Se (.51)
Sm (.82)	La (.90)	Eu (.89)	Eu (.36)
Lu (.79)	Eu (.84)	Lu (.84)	Lu (.13)
Ce (.74)	Lu (.84)	La (.81)	negative

Table 6. Sample locations and associations.

Sample	Location	Spatial association
120-A	Vale de Ermide 13 W, vug 120	same vug
120-B	Vale de Ermide 13W, vug 120	same vug
120-C	Vale de Ermide 13W, vug 120	same vug
120-D	Vale de Ermide 13W, vug 120	same vug
303	D15 R15 AW10 Level 0, pillar 194	different pillar
298	D15 R15 AW10 Level 0, pillar ?	different pillar
277	D15 R15 AW10 Level 1,	different level
290	D15 R15 AW10 Level 0, pillar 56	same pillar
291	D15 R15 AW10 Level 0, pillar 56	same pillar
241	D15 R9 AW13 Level 1	different pillar
248	D15 R9 AW13 Level 1	different pillar
216	D9 R19 Level 0	different pillar
226	D9 R19 Level 0	different pillar
203	D7 R21 14W Level 0	different stope
207-A	D7 R19 AW10 Level 0, vug 207	same vug
207-B	D7 R19 AW10 Level 0, vug 207	same vug
207-C	D7 R19 AW10 Level 0, vug 207	same vug
207-B	D7 R19 AW10 Level 0, vug 207	same vug

sible. Just as Band 4 does not correlate with the other emission bands, selenium does not correlate with the REE.

Table 5 summarizes the statistical data. Based on these observations and the literature described above, the following relations are a summary of our conclusions regarding causes of luminescence:

Band 1 (349 nm); REE activation, possibly Ce^{3+}
Band 2 (445 nm); REE activation, possibly Eu^{2+}
Band 3 (555 nm); Mn^{2+} activation with REE sensitization, possibly Ce^{3+} and Eu^{2+}
Band 4 (701 nm); unknown activator

Using polarospectrography, Lagerwey (1977) interpreted emissions in Panasqueira apatites at 430–450 nm and 580 nm as related to Mn^{2+} and Eu^{2+}, respectively. He suggested that the transfer of energy from ions such as Ce^{3+} and Eu^{2+} enhanced the emission of the activators. The results of our investigation support his interpretations.

Observational evidence for models. Qualitative support for the model of manganese luminescence sensitized by europium and cerium was demonstrated in photographs taken of the test crystal with the filtering techniques used earlier for quantification of emission intensity. The resulting series of four photographs (Fig. 4) reveals that zones 5+ and 4 are visible only on the photographs recording Band 3 (Mn) and Band 4 (?) emission; Band 1 (Ce) and Band 2 (Eu) emissions are lacking. The Mn/Ce and Mn/Eu ratios for zones 5+ and 4 are significantly higher than in the other luminescent zones. Mn/Ce ratios for zones 5+ and 4 are 40 and 96, respectively, compared to less than 20 for other zones. Mn/Eu ratios are 254 and 289, respectively, compared to less than 30 for the other zones. Evidently at high Mn/REE ratios, manganese absorption of the REE energy is complete.

Fission track production

The test crystal was cut perpendicular to the c-axis, polished, etched with 5% HNO_3 for 30 seconds, and examined for fission tracks. Under high magnification the hexagonal fission track pits could be easily distinguished from other pits by randomly oriented tails of the former (Kelly and Wagner, 1977). Track densities were estimated by counting the number of tracks observed in the field of view at $800\times$ magnification and ranged from 760–3800 tracks/mm². Fission track density was generally, but not consistently, higher in zones distinguished by a dark green color.

For the zones that had been analyzed by NAA a strong correlation between track density and uranium concentration (R = 0.81) was observed. The strong correlation between fission track density and uranium concentration, supports the accuracy of the neutron activation analyses.

Fission tracks are sites of crystal defects. To determine whether these defects affect the luminescence or color of the apatites, a crystal was annealed in an oven for 7 days at 410°C. Complete erasure of the tracks produced no observable change in the luminescence or color of the crystal, indicating that the fission track defects are unrelated to these properties.

Color

The causes of color in apatites are incompletely understood (McConnel, 1973). This study is not rigorously spectroscopic in design and cannot be definitive in result, but does lead to some interesting speculation concerning the color zonation of the Panasqueira apatites. We observed that the color of the apatites, dark green to colorless, is not related to the crystal defects associated with the fission tracks. Color is, in fact, related to luminescence; the zones of strongest luminescence (highest REE concentration) were the most devoid of color. We suggest that these apatites in their common state are green (the most plausible chromaphore being Fe^{2+}), but when enriched in REE they become colorless. The decolorizing mechanism could be oxidation of the chromaphore or, more importantly, complimentary absorption. REE, generally Nd^{3+} or Ce^{3+}, are used as complimentary absorbers in the glass industry to decolorize green glass (Weyl, 1959). Detailed absorption spectroscopic measurements could test this hypothesis for the Panasqueira apatites.

Stratigraphic correlation

Growth stratigraphies were described by logging techniques for 18 crystals collected at scattered locations in the Barroca Grande and Vale da Ermida sections of the mine. The crystals came from the same, interconnected vein system, and formed during the same stage of vein filling. As indicated in Table 3, some of these crystals came from the same vug whereas others were separated by distances of almost one kilometer. It was not possible to trace or correlate the sampled veins from one sampling site to the next. Indeed, a motivation for this study was to determine if the apatite "stratigraphy" could be used to establish temporal and spatial relationships within the vein system.

Luminescence logging

Each crystal was photographed using a UV filter under irradiation by a high pressure Hg-lamp. The observed zo-
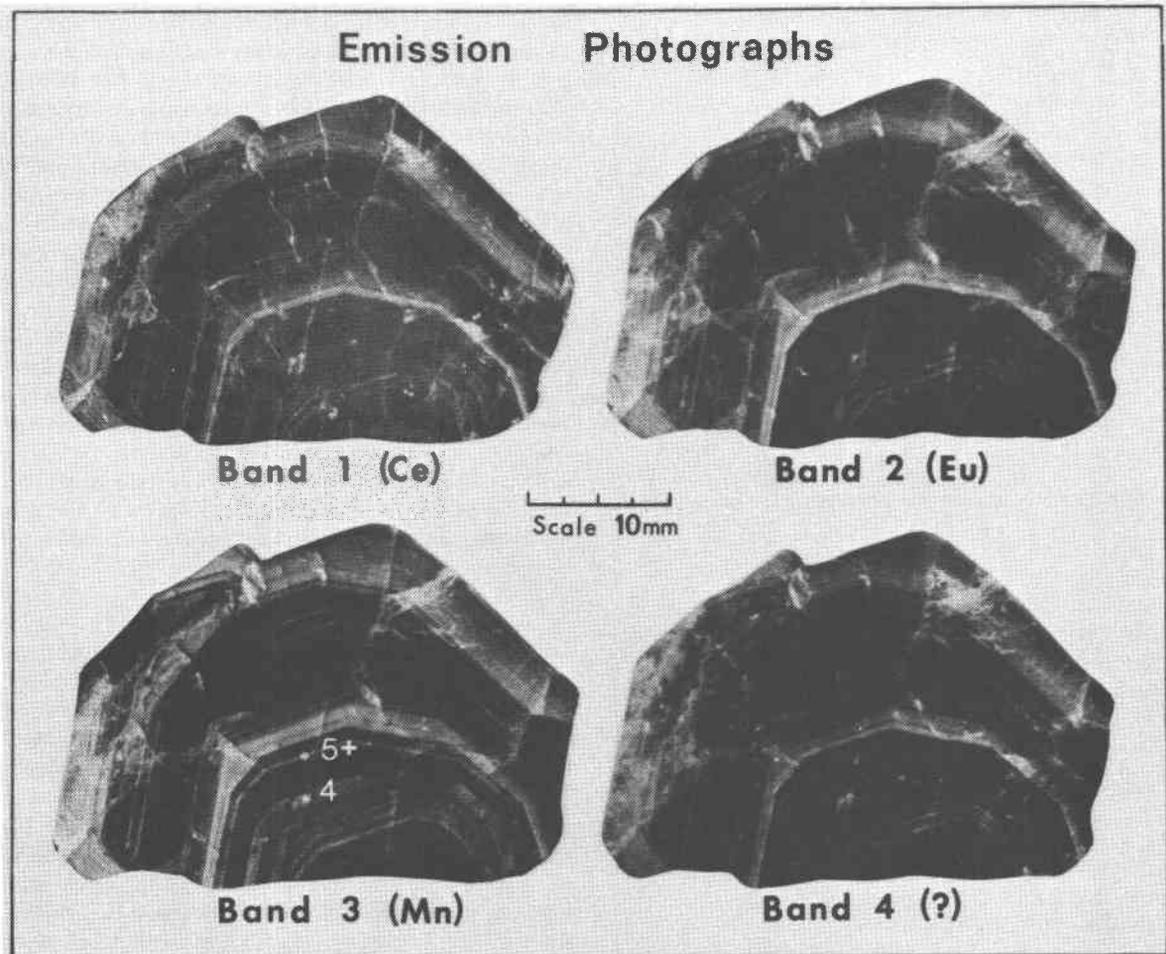
Fig. 4. Luminescence patterns of each of the characteristic emission bands. Note the absence of zones 5+ and 4 in the cerium and europium emission photographs.

nation patterns (e.g., Fig. 1) were characterized by placing enlarged positives on a light table and photometrically recording the relative intensity of light transmitted through the photograph along radial traverses.

Fission track logging

Microscope traverses were made across each polished and etched crystal. Spatial orientation was determined in relation to the luminescent bands. Track density was estimated as previously described.

Results

The resulting crystal stratigraphies are shown in Figure 5. The dotted lines represent fission track density (uranium concentration), and the solid lines represent luminescence intensity (REE concentration). The vertical axis indicates translation along the radial traverse. The dimension of this vertical axis is arbitrary; downwards is toward the crystal core. The horizontal axis is a relative scale of emission intensity and fission track density. Luminescence intensity

generally varies independently of fission track density, but notable exceptions are samples 120-A, B and C. For those samples there is a clear correlation between increased luminescence intensity and low fission track density; i.e., REE and uranium concentrations appear to be negatively correlated. The statistical data for the test crystal exhibit no such relation, however. In addition, the negative correlation is valid only for selected regions of some samples. The fission track logs are usually less variable than the luminescence logs, indicating that incorporation of uranium into the apatite structure was less variable with time than incorporation of REE.

The "stratigraphies" were compared visually to determine whether the results for any crystals could be correlated. Crystal correlation was assumed if the stratigraphies were similar. For example, crystals 120-A, B and C which came from the same 3 meter long vug, show clearly correlative stratigraphies. The luminescence log of each of the three crystals is characterized by a strongly fluorescent rim and core separated by a wide band of low intensity lumine-
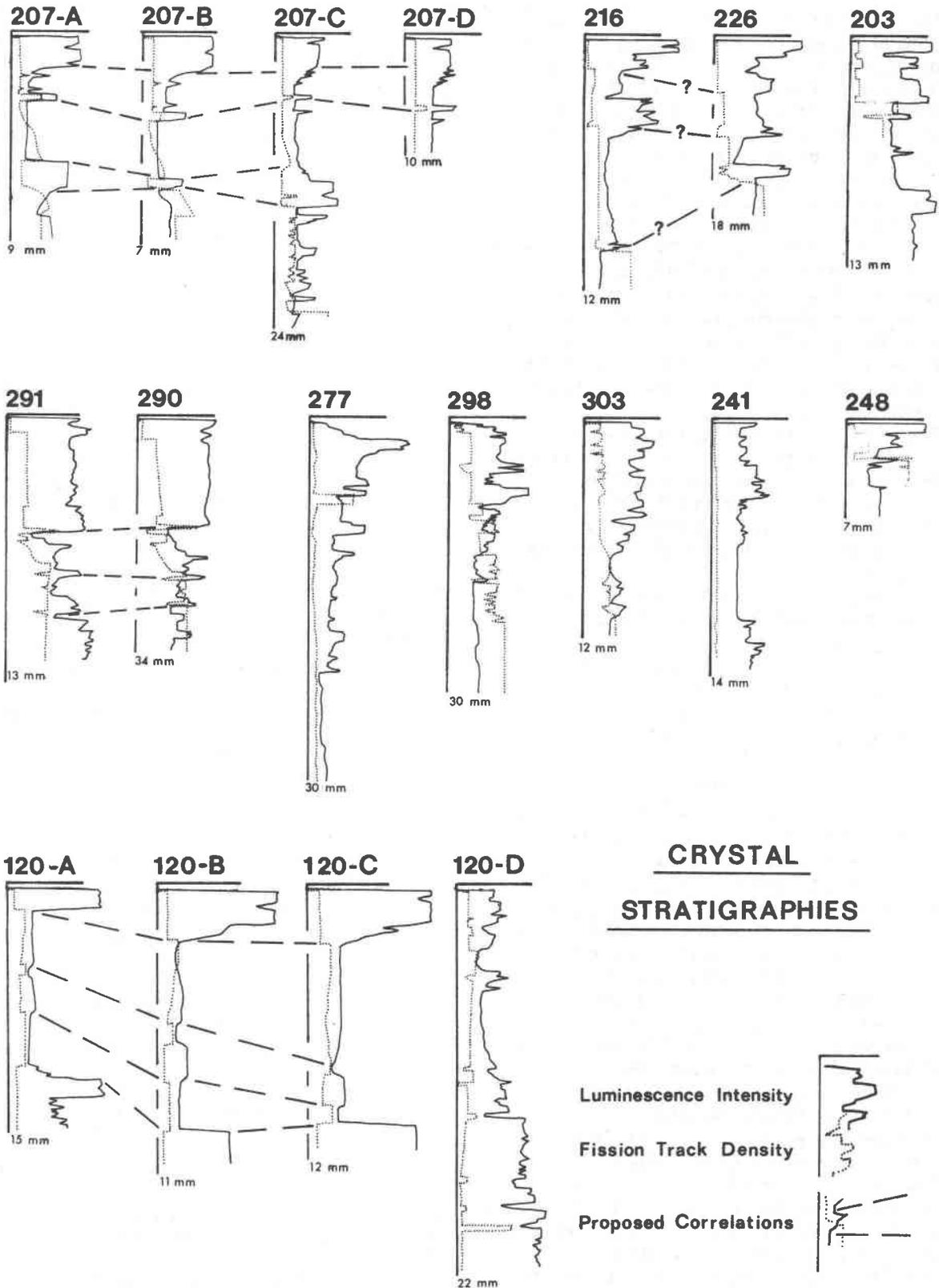
Fig. 5. Crystal "stratigraphies" as described by the fission track and luminescence logs. Proposed correlations are indicated. The scale is noted for each crystal traverse.

scence in which occur two diffuse, yet distinctly divided, fluorescent bands. The fission track log for each crystal varies in a manner similar to the luminescence log, but the variation is less in magnitude and opposite in direction. All of the crystal stratigraphies were examined in this manner. Generally, similarities were more readily observable between the fission track logs than the luminescence logs. The combined variation of the two logs, however, was always used to substantiate proposed correlations.

Comparison of the crystal stratigraphies revealed positive correlations between crystals from the same vug (samples 120-A, B and C, but not 120-D) and the same vein exposed in a single, 5 meter long pillar (samples 290 and 291), but the correlations appear to break down at larger sample spacings. With only one possible exception (samples 216 and 226), there is no convincing correlation of apatite stratigraphy in crystals occurring in separate pillars 10 meters or more apart.

The limited spatial extent of correlative apatite stratigraphies is not entirely surprising in view of the multiple controls of the independent fission track density and luminescence intensity which were both used to define zoning in any single crystal. Small variations in the proportions of trace uranium and REE in the apatites would cause large variations in these parameters. These variations in trace elements in the apatites probably reflect chemical inhomogeneities of the fluids from which they formed, but the differences could be slight, and it is uncertain whether they indicate local compositional gradients in fluids with a more-or-less uniform flow direction, or the existence of a more complex flow regime involving local, compositionally different hydrologic cells.

Discussion

The crystal zonation of the Panasqueira apatites is a function of REE and uranium distributions. Incorporation of these ions into the apatite structure depends on the concentration of the relative complexes in the ore fluid and on the partitioning coefficients of the apatite and co-precipitating minerals. At a fixed point in the vein system, the ore fluid undergoes chemical changes related to ore–fluid evolution, to fluid–wallrock reaction, and to variations in the hydrologic regime. Because incorporation of U and REE into the apatite structure is sensitive to these chemical variations, the zonation of the apatites represents both local flow perturbations and temporal variations of the ore fluid. One would expect that if the flow regime of a vein system is significantly complex, the zonation related to local spatial changes would overlap and effectively mask the zonation related to temporal variations.

Examination of the apatite crystal stratigraphies demonstrates that even the open vein system at Panasqueira has a flow regime sufficiently complex to mask temporal variations. Similarities between crystal stratigraphies are observed only locally, indicating that the primary controls of crystal zonation were local. Numerous mechanisms, ranging from local trace element partitioning among coprecipi-

tating phases to the existence of compositionally different hydrologic cells, could be proposed to explain the apatite stratigraphies recorded. Even though these studies did not permit correlation of an ordered stratigraphy in the Panasqueira apatites over widely spaced areas of the deposit, this description of the techniques hopefully will lead to more successful applications in more cooperative apatite-bearing deposits.

References

Barton, P. B., Jr., Bethke, P. M. and Roedder, E. (1977) Environment of ore deposition in the Creede mining district, San Juan Mountains, Colorado: Part III, Progress toward interpretation of the chemistry of the ore forming fluids of the OH vein. Economic Geology, 72, 1–24.

Bloot, C. and de Wolf, L. C. M. (1953) Geologic features of the Panasqueira tin-tungsten ore occurrence. Boletim Sociedade Geologica de Portugal, 11, 1–58.

Botden, P. J. (1952) Transfer and transport of energy by resonance processes in luminescent solids. Philips Research Reporter, 7, 198–235.

Buerger, M. J. (1960) Crystal-Structure Analyses. J. Wiley and Sons, Inc., New York.

Flaningan, F. H. (1973) 1972 Values for international geochemical reference samples. Geochimica et Cosmochimica Acta, 37, 1189–1200.

Gaines, R. V. and Thadeu, D. (1971) The minerals of Panasqueira, Portugal. Mineralogical Record, 2, 73–78.

Goldberg, P. (1966) Luminescence of Inorganic Solids. Academic Press, New York.

Gorobets, B. S. (1968) On the luminescence of fluorapatites activated by RE elements. Optics and Spectroscopy, 25, 154–155.

Kallman, H. P. and Spruch, G. M. (1962) Luminescence of Organic and Inorganic Materials, J. Wiley and Sons, Inc., New York.

Kelly, W. C. and Rye, R. O. (1979) Geologic, fluid inclusion, and stable isotope studies of the tin-tungsten deposits of Panasqueira, Portugal. Economic Geology, 74, 1721–1823.

Kelly, W. C. and Wagner, G. A. (1977) Paleothermometry by combined application of fluid inclusion and fission track methods. Neues Jahrbuch für Mineralogie Monatschefte, 1–15.

Lagerwey, A. A. F. (1977) Detection of trace elements in apatite crystals from Panasqueira, Portugal by non-destructive optical methods, especially polarspectrography. Scripta Geologica, #42, Leiden.

Leckebusch, R. (1979) Comments on the luminescence of apatites from Panasqueira, Portugal. Neues Jahrbuch für Mineralogie, Monatschefte, 17–21.

Mariano, A. N. and Ring, P. J. (1975) Europium activated cathodoluminescence in minerals. Geochimica et Cosmochimica Acta, 39, 649–660.

McConnel, D. (1973) Apatite. Springer-Verlag, New York.

McLimans, R. K., Barnes, H. L. and Ohmoto, H. (1980) Sphalerite stratigraphy of the Upper Mississippi Valley zinc-lead district. Economic Geology, 75, 351–361.

Portnov, A. M. and Gorobets, B. S. (1969) Luminescence of apatites from different rock types. Seriya Geologischeskaya, 184, 110–113.

Roedder, E. (1969) Variable banding of possible annual origin in celestite crystals from Clay Center, Ohio, and in other minerals. American Mineralogist, 54, 789–810.

Rucklidge, J. C. and Gasparrini, E. L. (1969) Specifications of a Complete Program for Processing Electron Microprobe Data: EMPADR VII. Department of Geology, University of Toronto.

Taraschan, A. N. (1969) Nature of luminescence in apatites (in Russian), Izvestiya Akademii Nauk SSR. Doklady of the Academy of Sciences of the USSR, Earth Sciences Sections.

Thadeu, D. (1951) Geologia do couto mineiro da Panasqueira (in Portuguese), Communicoes dos Servisos Geolgogicos de Portugal, 32, 50–64.

Van Uitert, L. G. (1966) Mechanisms of energy transfer involving tri-valent Sm, Eu, Tb, Dy and Yb. Proceedings of the International Conference on Luminescence, 1588–1603.

Weyl, W. A. (1959) Colored Glasses. Dawsons of Pall Mall, London.